

Detecting extrasolar planets from stellar radial velocities using Bayesian evidence

F. Feroz^{*}, S. T. Balan and M. P. Hobson

Astrophysics Group, Cavendish Laboratory, JJ Thomson Avenue, Cambridge CB3 0HE, UK

Accepted —. Received —; in original form 6 November 2018

ABSTRACT

Stellar radial velocity (RV) measurements have proven to be a very successful method for detecting extrasolar planets. Analysing RV data to determine the parameters of the extrasolar planets is a significant statistical challenge owing to the presence of multiple planets and various degeneracies between orbital parameters. Determining the number of planets favoured by the observed data is an even more difficult task. Bayesian model selection provides a mathematically rigorous solution to this problem by calculating marginal posterior probabilities of models with different number of planets, but the use of this method in extrasolar planetary searches has been hampered by the computational cost of the evaluating Bayesian evidence. Nonetheless, Bayesian model selection has the potential to improve the interpretation of existing observational data and possibly detect yet undiscovered planets. We present a new and efficient Bayesian method for determining the number of extrasolar planets, as well as for inferring their orbital parameters, without having to calculate directly the Bayesian evidence for models containing a large number of planets. Instead, we work iteratively and at each iteration obtain a conservative lower limit on the odds ratio for the inclusion of an additional planet into the model. We apply this method to simulated data-sets containing one and two planets and successfully recover the correct number of planets and reliable constraints on the orbital parameters. We also apply our method to RV measurements of HD 37124, 47 Ursae Majoris and HD 10180. For HD 37124, we confirm that the current data strongly favour a three-planet system. We find strong evidence for the presence of a fourth planet in 47 Ursae Majoris, but its orbital period is suspiciously close to one year, casting doubt on its validity. For HD 10180 we find strong evidence for a six-planet system.

Key words:

stars: planetary systems – stars: individual: HD 37124 – stars: individual: 47 Ursae Majoris – stars: individual: HD 10180 – techniques: radial velocities – methods: data analysis – methods: statistical

1 INTRODUCTION

Extrasolar planetary research has been revitalised in the last decade and so far more than 500 extrasolar planets have been discovered. Improvements in the accuracy of RV measurements have made it possible to detect planets with larger orbital periods and smaller velocity amplitudes. With the flood of new data, more powerful statistical techniques are being developed and applied to extract as much information as possible. Traditionally, planet parameters and their uncertainties were obtained by searching for periodicity in the RV data using the Lomb-Scargle periodogram (Lomb 1976; Scargle 1982) to fix the orbital period and then estimating other parameters by using minimisation algorithms.

Recent advances in Marko-Chain Monte Carlo (MCMC) tech-

niques (see e.g. Mackay 2003) have made it possible for Bayesian techniques to be applied to extrasolar planetary searches (see e.g. Gregory 2005; Ford 2005; Ford & Gregory 2007; Balan & Lahav 2009). Bayesian methods have several advantages over traditional methods, for example when the data do not cover a complete orbital phase of the planet. Bayesian inference also provides a rigorous way of performing model selection which is required to decide the number of planets favoured by the data. The main problem in applying such Bayesian model selection techniques is the computational cost involved in calculating the Bayesian evidence (see Sec. 2).

Clyde et al. (2007) recently reviewed the state of techniques for model selection from a statistical perspective and Ford & Gregory (2007) evaluated the performance of a variety of marginal likelihood estimators in the extrasolar planet context. Gregory (2007b) found good agreement (within 28%) be-

^{*} E-mail: f.feroz@mrao.cam.ac.uk

tween three estimators: (a) parallel tempering, (b) the ratio estimator, and (c) Restricted Monte Carlo (RMC) for one and two planet models. However, for a 3 planet model the three estimators diverged significantly with the RMC yielding the lowest estimate. Gregory & Fischer (2010) introduced the Nested Restricted Monte Carlo (NMRC) estimator, an improvement on the RMC estimator. The NRMC estimator is expected to provide a conservative lower bound on the Bayesian evidence in higher dimensions. These Bayesian model selection techniques have already resulted in the discovery of previously unknown planets in existing datasets, e.g. Tuomi & Kotiranta (2009) discovered a second planet orbiting HD 11506 and Gregory & Fischer (2010) reported a third planet orbiting 47 Ursae Majoris using Bayesian analysis. Nevertheless, most of the Bayesian model selection techniques employed so far in extrasolar planetary searches have relied on estimates of the Bayesian evidence, with uncertain accuracy. Our aim in this paper is to present a new and efficient method for Bayesian model selection to determine the number of planets favoured by the data, and estimate their parameters, *without* having to calculate directly the Bayesian evidence for models containing a large number of planets.

The outline of this paper is as follows. We give a brief introduction to Bayesian inference in Sec. 2 and describe various Bayesian object detection techniques in Sec. 3. Our model for calculating radial velocities is described in Sec. 4. In Sec. 5 we describe our Bayesian analysis methodology including the descriptions of likelihood and prior probability functions. We apply our method to simulated data in Sec. 6, and to real RV data sets on HD 37124, 47 Ursae Majoris and HD 10180 in Sec. 7. Finally our conclusions are presented in Sec. 8.

2 BAYESIAN INFERENCE

Our planet finding methodology is built upon the principles of Bayesian inference, and so we begin by giving a brief summary of this framework. Bayesian inference methods provide a consistent approach to the estimation of a set of parameters Θ in a model (or hypothesis) H for the data \mathbf{D} . Bayes' theorem states that

$$\Pr(\Theta|\mathbf{D}, H) = \frac{\Pr(\mathbf{D}|\Theta, H) \Pr(\Theta|H)}{\Pr(\mathbf{D}|H)}, \quad (1)$$

where $\Pr(\Theta|\mathbf{D}, H) \equiv P(\Theta)$ is the posterior probability distribution of the parameters, $\Pr(\mathbf{D}|\Theta, H) \equiv \mathcal{L}(\Theta)$ is the likelihood, $\Pr(\Theta|H) \equiv \pi(\Theta)$ is the prior, and $\Pr(\mathbf{D}|H) \equiv \mathcal{Z}$ is the Bayesian evidence.

In parameter estimation, the normalising evidence factor is usually ignored, since it is independent of the parameters Θ , and inferences are obtained by taking samples from the (unnormalised) posterior using standard MCMC sampling methods, where at equilibrium the chain contains a set of samples from the parameter space distributed according to the posterior. This posterior constitutes the complete Bayesian inference of the parameter values, and can be marginalised over each parameter to obtain individual parameter constraints.

In contrast to parameter estimation problems, for model selection the evidence takes the central role and is simply the factor required to normalize the posterior over Θ :

$$\mathcal{Z} = \int \mathcal{L}(\Theta) \pi(\Theta) d^D \Theta, \quad (2)$$

where D is the dimensionality of the parameter space. As the average of the likelihood over the prior, the evidence is larger for

$ \Delta \ln R $	Odds	Probability	Remark
< 1.0	$\lesssim 3 : 1$	< 0.750	Inconclusive
1.0	$\sim 3 : 1$	0.750	Weak Evidence
2.5	$\sim 12 : 1$	0.923	Moderate Evidence
5.0	$\sim 150 : 1$	0.993	Strong Evidence

Table 1. The scale we use for the interpretation of model probabilities.

a model if more of its parameter space is likely and smaller for a model with large areas in its parameter space having low likelihood values, even if the likelihood function is very highly peaked. Thus, the evidence automatically implements Occam's razor: a simpler theory with compact parameter space will have a larger evidence than a more complicated one, unless the latter is significantly better at explaining the data. The question of model selection between two models H_0 and H_1 can then be decided by comparing their respective posterior probabilities given the observed data set \mathbf{D} , as follows

$$R = \frac{\Pr(H_1|\mathbf{D})}{\Pr(H_0|\mathbf{D})} = \frac{\Pr(\mathbf{D}|H_1) \Pr(H_1)}{\Pr(\mathbf{D}|H_0) \Pr(H_0)} = \frac{\mathcal{Z}_1 \Pr(H_1)}{\mathcal{Z}_0 \Pr(H_0)}, \quad (3)$$

where $\Pr(H_1)/\Pr(H_0)$ is the a priori probability ratio for the two models, which can often be set to unity but occasionally requires further consideration. The natural logarithm of the ratio of posterior model probabilities (sometimes termed the posterior odds ratio) provides a useful guide to what constitutes a significant difference between two models:

$$\Delta \ln R = \ln \left[\frac{\Pr(H_1|\mathbf{D})}{\Pr(H_0|\mathbf{D})} \right] = \ln \left[\frac{\mathcal{Z}_1 \Pr(H_1)}{\mathcal{Z}_0 \Pr(H_0)} \right]. \quad (4)$$

We summarize the convention usually used for model selection in Table 1.

Evaluation of the multidimensional integral in Eq. 2 is a challenging numerical task. Standard techniques like thermodynamic integration are extremely computationally expensive which makes evidence evaluation at least an order of magnitude more costly than parameter estimation. Some fast approximate methods have been used for evidence evaluation, such as treating the posterior as a multivariate Gaussian centred at its peak (see e.g. Hobson & McLachlan 2003), but this approximation is clearly a poor one for multimodal posteriors (except perhaps if one performs a separate Gaussian approximation at each mode). The Savage-Dickey density ratio has also been proposed (see e.g. Trotta 2007) as an exact, and potentially faster, means of evaluating evidences, but is restricted to the special case of nested hypotheses and a separable prior on the model parameters. Various alternative information criteria for astrophysical model selection are discussed by Liddle (2007), but the evidence remains the preferred method.

The nested sampling approach, introduced by Skilling (2004), is a Monte Carlo method targeted at the efficient calculation of the evidence, but also produces posterior inferences as a by-product. Feroz & Hobson (2008) and Feroz et al. (2009b) built on this nested sampling framework and have recently introduced the MULTINEST algorithm which is very efficient in sampling from posteriors that may contain multiple modes and/or large (curving) degeneracies and also calculates the evidence. This technique has greatly reduced the computational cost of Bayesian parameter estimation and model selection and has already been applied to several model selections problem in astrophysics (see e.g. Feroz et al. 2008, 2009c,a). We employ this technique in this paper.

3 BAYESIAN OBJECT DETECTION

To detect and characterise an unknown number of objects in a dataset the Bayesian purist would attempt to infer simultaneously the full set of parameters $\Theta = \{N_{\text{obj}}, \Theta_1, \Theta_2, \dots, \Theta_{N_{\text{obj}}}, \Theta_n\}$, where N_{obj} is the (unknown) number of objects, Θ_i are the parameters values associated with the i th object, and Θ_n is the set of (nuisance) parameters common to all the objects. In particular, this approach allows for the inclusion of an informative prior (if available) on N_{obj} . The crucial complication inherent in this approach, however, is that the dimensionality of parameter space is variable and therefore the analysis method should be able to move between spaces of different dimensionality. Such techniques are discussed in Hobson & McLachlan (2003). Nevertheless, due to this additional complexity of variable dimensionality, the techniques are generally extremely computationally intensive.

An alternative and algorithmically simpler approach for achieving virtually the same result ‘by hand’ is instead to consider a *series* of models $H_{N_{\text{obj}}}$, each with a *fixed* number of objects, i.e. with $N_{\text{obj}} = 0, 1, 2, \dots$. One then infers N_{obs} by identifying the model with the largest marginal posterior probability $\text{Pr}(H_{N_{\text{obj}}}|\mathbf{D})$. The probability associated with $N_{\text{obj}} = 0$ is often called the ‘null evidence’ and provides a baseline for comparison of different models. Indeed, this approach has been adopted previously in exoplanet studies (see e.g. Gregory & Fischer (2010)), albeit using only lower-bound estimates of the Bayesian evidence for each model. Assuming that there are n_p parameters per object and n_n (nuisance) parameters common to all the objects, for N_{obj} objects, there would be $N_{\text{obj}}n_p + n_n$ parameters to be inferred. Thus, the dimensionality of the problem and consequently the volume of the parameter space increases almost linearly with N_{obj} . Along with this increase in dimensionality, the complexity of the problem also increases due to exponential increase in the number of modes as a result of counting degeneracy, e.g. for $N_{\text{obj}} = 2$ and $\Theta = \{\Theta_1, \Theta_2, \Theta_n\}$ where Θ_1 and Θ_2 are the parameters values associated with first and second objects respectively and Θ_n is the set of nuisance parameters, one would get the same value for the likelihood $\mathcal{L}(\Theta)$ by just rearranging Θ as $\{\Theta_2, \Theta_1, \Theta_n\}$ and therefore there should at least be twice as many modes for $N_{\text{obj}} = 2$ than for $N_{\text{obj}} = 1$. Similarly there are $n!$ more modes for $N_{\text{obj}} = n$ than for $N_{\text{obj}} = 1$. This increase in dimensionality and severe complexity of the posterior makes it very difficult to evaluate the Bayesian evidence, even approximately. In exoplanet analyses, we have found that MULTINEST is typically capable of evaluating the evidence accurately for systems with up to 3 planets. If 4 or more planets are present, MULTINEST still maps out the posterior distribution sufficiently well to obtain reliable parameter estimates, but can begin to produce inaccurate evidence estimates. Thus, even this approach to Bayesian object detection is of limited applicability in exoplanet studies.

If the contributions to the data from each object are reasonably well separated and the correlations between parameters across objects is minimal, one can use the alternative approach of setting $N_{\text{obj}} = 1$ (see. e.g. Hobson & McLachlan 2003; Feroz & Hobson 2008) and therefore the model for the data consists of only a single object. This does not, however, restrict us to detecting only one object in the data. By modelling the data in such a way, we would expect the posterior distribution to possess numerous peaks, each corresponding to the location of one of the objects. Consequently the high dimensionality of the problem is traded with high multi-modality in this approach, which, depending on the statistical method employed for exploring the parameter space, could poten-

tially simplify the problem enormously. For an application of this approach in detecting galaxy cluster from weak lensing data-sets see Feroz et al. (2008). Unfortunately, for extrasolar planet detection using RV, this approach cannot be utilized as the nature of data itself makes the parameters of different planets in multi-planet system correlated.

We therefore propose here a new general approach to Bayesian object detection that is applicable to exoplanet studies, even for systems with a large number of planets. Motivated by the fact that, as discussed above and in Sec. 2, evaluation of the evidence integral is a far more computationally demanding procedure than parameter estimation, we consider a method based on the analysis of residuals remaining after detection and subsequent inclusion in the model of N_{obj} objects from the data, as outlined below. In what follows, we will simply assume that the prior ratio in Eq. 4 is unity, so that the posterior odds ratio R coincides with the evidence ratio. In principle, however, one could adopt a more informative prior ratio given a theory of planet formation that predicted the probability distribution for the number of planets.

Our approach to Bayesian object detection is as follows. Let us first denote the observed (fixed) data by $\mathbf{D} = \{d_1, d_2, \dots, d_M\}$, with the associated uncertainties being $\{\sigma_1, \sigma_2, \dots, \sigma_M\}$. In the general case that $N_{\text{obj}} = n$, let us define the random variable \mathbf{D}_n as the data that would be collected if the model H_n were correct, and also the random variable $\mathbf{R}_n \equiv \mathbf{D} - \mathbf{D}_n$, which are the data residuals in this case. If we set $N_{\text{obj}} = n$ and analyse \mathbf{D} to obtain samples from the posterior distribution of the model parameters Θ , using MULTINEST, then from these samples it is straightforward to obtain samples from the posterior distribution of the data residuals \mathbf{R}_n . This is given by

$$\text{Pr}(\mathbf{R}_n|\mathbf{D}, H_n) = \int \text{Pr}(\mathbf{R}_n|\Theta, H_n) \text{Pr}(\Theta|\mathbf{D}, H_n) d\Theta, \quad (5)$$

where

$$\text{Pr}(\mathbf{R}_n|\Theta, H_n) = \prod_{i=1}^M \frac{1}{\sqrt{2\pi\sigma_i^2}} \exp\left\{-\frac{[D_i - R_i - D_{p,i}(\Theta)]^2}{2\sigma_i^2}\right\}, \quad (6)$$

and $\mathbf{D}_p(\Theta)$ is the (noiseless) predicted data-set corresponding to the parameter values Θ . It should be noted that (5) and (6) contain no approximations. In principle, one could then perform a kernel estimation procedure on the samples obtained to produce a (possibly analytic) functional form for $\text{Pr}(\mathbf{R}_n|\mathbf{D}, H)$. For simplicity, we assume here that the residuals are independently Gaussian distributed with a mean $\langle \mathbf{R}_n \rangle = \{r_1, r_2, \dots, r_M\}$ and standard deviations $\{\sigma'_1, \sigma'_2, \dots, \sigma'_M\}$ obtained from the samples; we find that this is a good approximation.

These residual data $\langle \mathbf{R}_n \rangle$, with associated uncertainties, can then be analysed with $N_{\text{obj}} = 0$, giving the ‘residual null evidence’ $Z_{r,0}$, which is compared with the evidence value $Z_{r,1}$ obtained by analysing $\langle \mathbf{R}_n \rangle$ with $N_{\text{obj}} = 1$. We denote the natural logarithm of the evidence ratio $Z_{r,1}/Z_{r,0}$ between these two models by $\Delta \ln Z_r$. We are thus comparing the model H_0 that the residual data does not contain an additional planet to the model H_1 in which an additional planet is favoured.

Our overall procedure is therefore as follows. We first set $N_{\text{obj}} = 1$ and analyse the original data set \mathbf{D} . If, in the analysis of the corresponding residuals data, H_1 is favoured over H_0 , then the original data \mathbf{D} are analysed with $N_{\text{obj}} = 2$ and the same process is repeated. In this way, N_{obj} is increased in the analysis of the original data \mathbf{D} , until H_0 is favoured over H_1 in the analysis of the corresponding residual data. The resulting value for N_{obj} gives the

number of objects favoured by the data. This approach thus only requires the Bayesian evidence to be calculated for $N_{\text{obj}} = 1$ model (and the $N_{\text{obj}} = 0$ model, which is trivial); this reduces the computational cost of the problem significantly. Moreover, in principle, this procedure is exact. The only approximation made here, for the sake of simplicity, is to assume that $\text{Pr}(\mathbf{R}_n | \mathbf{D}, H_n)$ takes the form of an uncorrelated multivariate Gaussian distribution.

In adopting this approach, our rationale is that, if the n -planet model is correct, the corresponding data residuals \mathbf{R}_n should be consistent with instrumental noise, perhaps including an additional stellar jitter contribution (see Section 5.1). In this case, the null hypothesis, H_0 , should be preferred over the alternative hypothesis, H_1 , since the latter supposes that some additional signal, not consistent with noise, is present in the data residuals. If H_1 is preferred, we take this as an indication of further planet signal(s) present in the data, and therefore re-analysis the *original* dataset \mathbf{D} using an $(n + 1)$ -planet model. In this way, we circumvent the problem that the inclusion of an additional planet to an n -planet model will inevitably affect the best-fit parameters for the original n -planet subset.

4 MODELLING RADIAL VELOCITIES

It is extremely difficult to observe planets at interstellar distances directly, since the planets only reflect the light incident on them from their host star and are consequently many times fainter. Nonetheless, the gravitational force between the planets and their host star results in the planets and star revolving around their common centre of mass. This produces doppler shifts in the spectrum of the host star according to its RV, the velocity along the line-of-sight to the observer. Several such measurements, usually over an extended period of time, can then be used to detect extrasolar planets.

Following the formalism given in Balan & Lahav (2009), for N_p planets and ignoring the planet-planet interactions, the RV at an instant t_i observed at j th observatory can be calculated as:

$$v(t_i, j) = V_j - \sum_{p=1}^{N_p} K_p [\sin(f_{i,p} + \varpi_p) + e_p \sin(\varpi_p)], \quad (7)$$

where

- V_j = systematic velocity with reference to j th observatory,
- K_p = velocity semi-amplitude of the p th planet,
- ϖ_p = longitude of periastron of the p th planet,
- $f_{i,p}$ = true anomaly of the p th planet,
- e_p = orbital eccentricity of the p th planet,
- P_p = orbital period of the p th planet,
- χ_p = fraction of an orbit of the p th planet, prior to the start of data taking, at which periastron occurred.

Note that $f_{i,p}$ is itself a function of e_p , P_p and χ_p . While there is unique mean line-of-sight velocity of the center of motion, it is important to have a different velocity reference V_j for each observatory/spectrograph pair, since the velocities are measured differentially relative to a reference frame specific to each observatory.

We also model the intrinsic stellar variability s ('jitter'), as a source of uncorrelated Gaussian noise in addition to the measurement uncertainties. Therefore for each planet we have five free parameters: K , ϖ , e , P and χ . In addition to these parameters there are two nuisance parameters V and s , common to all the planets.

These orbital parameters can then be used along with the stellar mass m_s to calculate the length a of the semi-major axis of the planet's orbit around the centre of mass and the planetary mass m as follows:

$$a_s \sin i = \frac{KP\sqrt{1-e^2}}{2\pi}, \quad (8)$$

$$m \sin i \approx \frac{Km_s^{\frac{2}{3}}P^{\frac{1}{3}}\sqrt{1-e^2}}{(2\pi G)^{\frac{1}{3}}}, \quad (9)$$

$$a \approx \frac{m_s a_s \sin i}{m \sin i}, \quad (10)$$

where a_s is the semi-major axis of the stellar orbit about the centre-of-mass and i is the angle between the direction normal to the planet's orbital plane and the observer's line of sight. Since i cannot be measured with RV data, only a lower bound on the planetary mass m can be estimated.

5 BAYESIAN ANALYSIS OF RADIAL VELOCITY MEASUREMENTS

There are several RV search programmes looking for extrasolar planets. The RV measurements consist of the time t_i of the i th observation, the measured RV v_i relative to a reference frame and the corresponding measurement uncertainty σ_i . These RV measurements can be analysed using Bayes' theorem given in Eq. 1 to obtain the posterior probability distributions of the model parameters discussed in the previous section. We now describe the form of the likelihood and prior probability distributions.

5.1 Likelihood function

As discussed in Gregory (2007a), the errors on RV measurements can be treated as Gaussian and therefore the likelihood function can be written as:

$$\mathcal{L}(\Theta) = \prod_i \frac{1}{\sqrt{2\pi(\sigma_i^2 + s^2)}} \exp\left[-\frac{(v(\Theta; t_i) - v_i)^2}{2(\sigma_i^2 + s^2)}\right], \quad (11)$$

where v_i and σ_i are the i^{th} RV measurement and its corresponding uncertainty respectively, $v(\Theta; t_i)$ is the predicted RV for the set of parameters Θ , and s is intrinsic stellar variability. A large value of s can also indicate the presence of additional planets, e.g. if a two-planet system is analysed with a single-planet model then the velocity variations introduced by the second planet would act like an additional noise term and therefore contribute to s .

5.2 Choice of priors

For parameter estimation, priors become largely irrelevant once the data are sufficiently constraining, but for model selection the prior dependence always remains. Therefore, it is important that priors are selected based on physical considerations. We follow the choice of priors given in Gregory (2007a), as shown in Table 2.

The modified Jeffreys prior,

$$\text{Pr}(\theta|H) = \frac{1}{(\theta + \theta_0) \ln(1 + \theta_{\text{max}}/\theta_0)}, \quad (12)$$

behaves like a uniform prior for $\theta \ll \theta_0$ and like a Jeffreys prior (uniform in log) for $\theta \gg \theta_0$. We set $K_0 = s_0 = 1$ m/s and $K_{\text{max}} = 2129$ m/s, which corresponds to a maximum planet-star mass ratio of 0.01.

Parameter	Prior	Mathematical Form	Lower Bound	Upper Bound
P (days)	Jeffreys	$\frac{1}{P \ln(P_{\max}/P_{\min})}$	0.2	365,000
K (m/s)	Mod. Jeffreys	$\frac{(K+K_0)^{-1}}{\ln(1+(K_{\max}/K_0)(P_{\min}/P_1)^{1/3}(1/\sqrt{1-e_1^2}))}$	0	$K_{\max}(P_{\min}/P_1)^{1/3}(1/\sqrt{1-e_1^2})$
V (m/s)	Uniform	$\frac{1}{V_{\min}-V_{\max}}$	$-K_{\max}$	K_{\max}
e	Uniform	1	0	1
ϖ (rad)	Uniform	$\frac{1}{2\pi}$	0	2π
χ	Uniform	1	0	1
s (m/s)	Mod. Jeffreys	$\frac{(s+s_0)^{-1}}{\ln(1+s_{\max}/s_0)}$	0	K_{\max}

Table 2. Prior probability distributions.

N_p	$\Delta \ln \mathcal{Z}$	$\Delta \ln \mathcal{Z}_r$	s (m/s)
1	82.29 ± 0.15	-1.33 ± 0.13	0.42 ± 0.35

Table 3. The evidence and jitter values for the 1-planet simulation.

6 APPLICATION TO SIMULATED DATA

In this section, we apply our method to two sets of simulations, one with only one planet in the data and the other with two planets. Our aim here is to test our new methodology for Bayesian object detection, in particular the use of the Bayesian evidence in determining the correct number of planets. In particular, we analyse the same simulations used in Balan & Lahav (2009), which were obtained by calculating the radial velocities using (7) for the 1-planet and 2-planet models respectively. Gaussian noise with $\mu = 0.0$ m/s and $\sigma = 2.0$ m/s was then added to the resultant radial velocities.

6.1 One-planet simulation

The evidence and jitter values obtained in the analysis of the 1-planet simulation are presented in Table 3. Here $\Delta \ln \mathcal{Z}$ denotes the natural logarithm of evidence ratio Z_{N_p}/Z_0 , where Z_0 is the evidence for $N_p = 0$. $\Delta \ln \mathcal{Z}_r$ is the natural logarithm of evidence ratio $Z_{N_r,1}/Z_{N_r,0}$ where $Z_{N_r,1}$ and $Z_{N_r,0}$ are the evidence values for analysing the residual data, after subtracting N_p planets, as discussed in Sec. 3, with 1 and 0 planets respectively. $\Delta \ln \mathcal{Z}$ therefore, gives the evidence in favour of N_p planets while $\Delta \ln \mathcal{Z}_r$ gives the evidence in favour of there being an additional planet after N_p planets have already been found and removed from the data. The evidence values listed in Table 3 should be compared with the scale given in Table 1. It is clear that there is overwhelming evidence for the presence of 1 planet in the data. The negative $\Delta \ln \mathcal{Z}_r$ value further indicates that there is no evidence for the presence of any additional planets. Furthermore, the logarithm of the evidence for the 2-planet model was calculated to be 81.73 ± 0.16 , which is lower than the logarithm of the evidence for the 1-planet model listed in Table 3, providing further support for the 1-planet model.

Adopting the 1-planet model, therefore, the resulting estimated parameter values are listed in Table 4 and are in excellent agreement with the true values used to generate the simulation.

6.2 Two-planet simulation

The evidence and jitter values obtained in the analysis of the 2-planet simulation are presented in Table 5. One can see that for

Parameter	True	Estimate
P (days)	700.00	705.09 ± 12.71
K (m/s)	60.00	60.39 ± 0.56
e	0.38	0.38 ± 0.01
ϖ (rad)	3.10	3.10 ± 0.03
χ	0.67	0.67 ± 0.05
V (m/s)	12.00	11.90 ± 0.45
s (m/s)	0.00	0.42 ± 0.35

Table 4. True and estimated parameter values for the 1-planet simulation. The estimated values are quoted as $\mu \pm \sigma$ where μ and σ are the posterior mean and standard deviation respectively.

N_p	$\Delta \ln \mathcal{Z}$	$\Delta \ln \mathcal{Z}_r$	s (m/s)
1	41.92 ± 0.14	14.82 ± 0.14	7.47 ± 1.13
2	67.31 ± 0.16	-1.45 ± 0.13	0.51 ± 0.41

Table 5. The evidence and jitter values for the 2-planet simulation.

$N_p = 1$, the evidence value is quite large but $\Delta \ln \mathcal{Z}_r$ gives a very clear indication of the presence of an additional planet. The jitter s for $N_p = 1$ is also quite large. The presence of a second planet is confirmed by $\Delta \ln \mathcal{Z}$ value for $N_p = 2$, which is almost 10 ln units higher than for $N_p = 1$. The logarithm of the evidence for the 3-planet model was calculated to be 66.29 ± 0.16 , which is lower than the 2-planet model (see Table. 1), thus indicating a preference for the latter. Furthermore, both $\Delta \ln \mathcal{Z}_r$ and s for $N_p = 2$ strongly suggest that no additional planet is present. Thus, adopting the 2-planet model, the estimated parameter values obtained are listed in Table 6. Once again they are in excellent agreement with the true values used to generate the simulation.

7 APPLICATION TO REAL DATA

In this section, we apply our Bayesian object detection technique to real RV measurements of HD 37124, 47 Ursae Majoris and HD 10180 and compare our results with those of previous analyses of these systems.

7.1 HD 37124

HD 37124 is a metal-poor G4 dwarf star at a distance of 33 pc with mass $0.85 \pm 0.02 M_{\odot}$ (Butler et al. 2006; Valenti & Fischer 2005).

Parameter	Planet 1		Planet 2	
	True	Estimate	True	Estimate
P (days)	700.00	708.76 ± 15.08	100.00	100.45 ± 0.54
K (m/s)	60.00	60.35 ± 0.62	10.00	10.20 ± 0.62
e	0.38	0.38 ± 0.02	0.18	0.19 ± 0.05
ϖ (rad)	3.10	3.11 ± 0.04	1.10	1.27 ± 0.40
χ	0.67	0.67 ± 0.06	0.17	0.16 ± 0.08
V (m/s)	12.00	11.80 ± 0.52		
s (m/s)	0.00	0.51 ± 0.41		

Table 6. True and estimated parameter values for the 2-planet simulation. The estimated values are quoted as $\mu \pm \sigma$ where μ and σ are the posterior mean and standard deviation respectively.

N_p	$\Delta \ln \mathcal{Z}_r$	s (m/s)
1	12.04 ± 0.15	13.21 ± 1.43
2	5.17 ± 0.15	7.24 ± 0.93
3	-1.62 ± 0.14	2.06 ± 0.84

Table 7. The evidence and jitter values for the system HD 37124.

The first planet orbiting HD 37124 was found by Vogt et al. (2000). Subsequently two further planets were found by Butler et al. (2003) and Vogt et al. (2005) respectively. We use the 52 RV measurements given in Vogt et al. (2005) for our analysis. The RV data is plotted in Fig. 1.

We follow the object detection methodology outlined in Sec. 3 and analyse the RV data, starting with $N_p = 1$ and increasing it until the residual evidence ratio $\Delta \ln \mathcal{Z}_r < 0$. The resulting evidence and jitter values are presented in Table 7. We can clearly see $N_p = 3$ is the favoured model, with both the residual evidence ratio and jitter values strongly implying no additional planets are contributing to the data. Adopting the 3-planet model, the estimated parameter values are listed in Table 8 while the 1-D marginalised posterior probability distributions are shown in Fig. 2. The mean RV curve for the 3-planet model is overlaid on the RV measurements in Fig. 1.

Comparing our parameter values with those given in

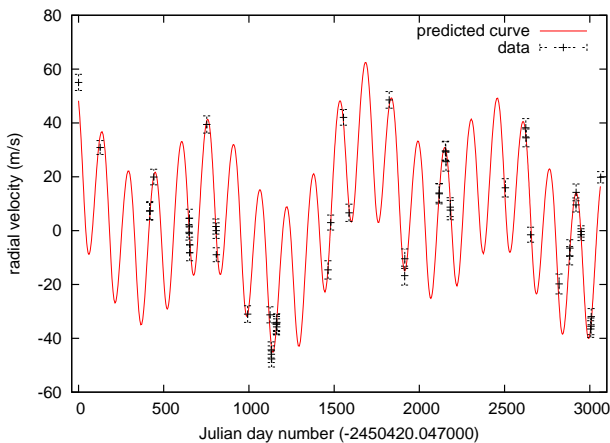


Figure 1. Radial velocity measurements, with 1σ errorbars, and the mean fitted radial velocity curve with three planets for HD 37124.

Parameter	HD 37124 b	HD 37124 c	HD 37124 d
P (days)	154.48 ± 0.14 (154.39)	853.70 ± 10.02 (855.22)	2195.48 ± 99.06 (2156.73)
K (m/s)	27.73 ± 1.06 (28.38)	14.16 ± 1.26 (14.15)	14.52 ± 1.96 (14.90)
e	0.07 ± 0.03 (0.10)	0.08 ± 0.06 (0.04)	0.43 ± 0.09 (0.45)
ϖ (rad)	1.41 ± 1.57 (0.70)	4.07 ± 1.58 (5.10)	3.47 ± 0.35 (3.78)
χ	0.72 ± 0.13 (0.74)	0.44 ± 0.35 (0.04)	0.29 ± 0.06 (0.25)
$m \sin i$ (M_J)	0.64 ± 0.02 (0.66)	0.58 ± 0.05 (0.58)	0.73 ± 0.07 (0.75)
a (AU)	0.53 ± 0.00 (0.53)	1.66 ± 0.01 (1.66)	3.11 ± 0.09 (3.08)

Table 8. Estimated parameter values for the three planets found orbiting HD 37124. The estimated values are quoted as $\mu \pm \sigma$ where μ and σ are the posterior mean and standard deviation respectively. The numbers in parenthesis are the maximum-likelihood parameter values.

N_p	$\Delta \ln \mathcal{Z}_r$	s (m/s)
1	98.27 ± 0.25	10.13 ± 0.47
2	23.32 ± 0.25	6.19 ± 0.36
3	4.39 ± 0.25	4.87 ± 0.33
4	-0.77 ± 0.23	4.35 ± 0.33

Table 9. The evidence and jitter values for the system 47 Ursae Majoris.

Vogt et al. (2005), we see that our parameter estimates for planets HD 37124 b and HD 37124 c are in very good agreement. However, our orbital time period for HD 37124 d is about 100 days lower and our estimated eccentricity is somewhat higher. The main reason for this discrepancy is that Vogt et al. (2005) fixed the eccentricity of HD 37124 d at 0.2 which was chosen to fulfill the dynamical stability requirement. Goździewski et al. (2006) also fitted a 3-planet model for HD 37124 and our parameter estimates for all three planets are in very good agreement with theirs.

7.2 47 Ursae Majoris

47 Ursae Majoris is a solar analog, yellow dwarf star at a distance of 14.06 pc with mass $1.06 \pm 0.02 M_\odot$ (Takeda et al. 2007). The first planet orbiting 47 Ursae Majoris with an orbital period of 1090 days was found by Butler & Marcy (1996). A second companion to 47 Ursae Majoris with orbital period of 2594 ± 90 days was discovered by Fischer et al. (2002). Subsequently the combined RV data for 47 Ursae Majoris from the Lick Observatory, spanning 21.6 years, and from the 9.2 m Hobby-Eberly Telescope (HET) and 12.7 m Harlam J. Smith (HJS) telescopes of the McDonald Observatory (Wittenmyer et al. 2009), was analysed by Gregory & Fischer (2010) and strong evidence was found in favour of a three-planet system. We analyse the same combined data-set. The RV data is plotted in Fig. 3.

Gregory & Fischer (2010) analysed the RV data this system by ignoring the residual velocity offsets associated with dewar changes, as well as by incorporating the dewar velocity offsets as additional unknown parameters, and found the results to be consistent. We therefore ignore the velocity offsets associated with dewar

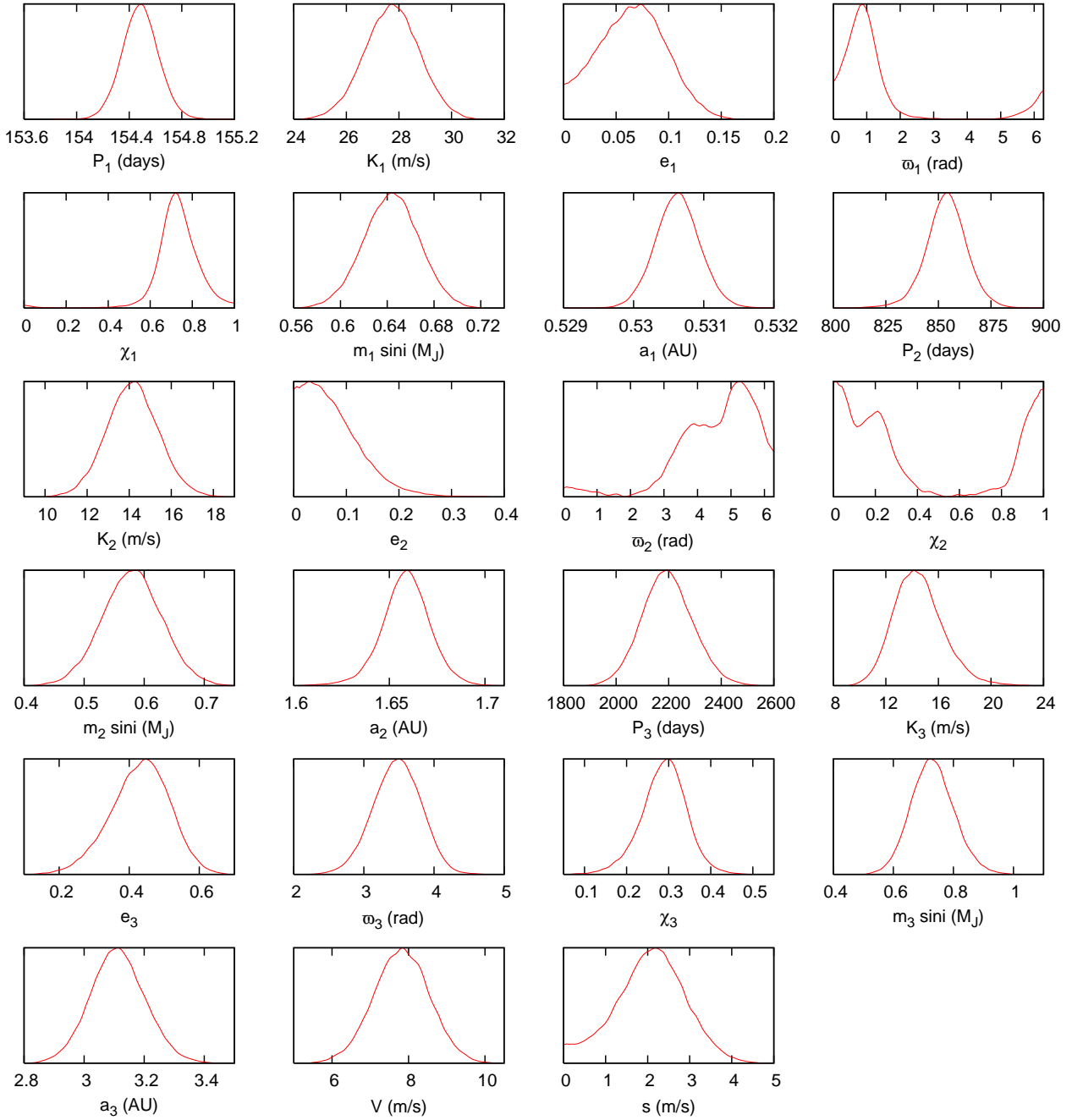


Figure 2. 1-D marginalised posterior probability distributions for the parameters of the three planets found orbiting HD 37124.

changes and fit for three velocity offsets V_L , V_{HET} and V_{HJS} associated with Lick, HET and HJS telescopes respectively.

We follow the object detection methodology outlined in Sec. 3 and analyse the RV data, starting with $N_p = 1$ and increasing it until the residual evidence ratio $\Delta \ln \mathcal{Z}_r < 0$. The resulting evidence and jitter values are presented in Table 9. We can clearly see $N_p = 4$ is the favoured model, with the residual evidence ratio strongly implying no additional planets are contributing to the data. Our detection of the fourth planet contradicts the analysis of Gregory & Fischer (2010), which did not find a well-defined peak for the fourth period using combined Lick, HET and HJS data-sets. They did, however, find the fourth planet using only the Lick data-

set, but their calculated upper limit on the false alarm probability for the presence of the fourth planet of ≈ 0.5 was deemed too high. Our detected fourth planet has the best-fit orbital period of 369.7 days, consistent with the period of fourth planet found by Gregory & Fischer (2010) in Lick-only data. Nonetheless, this period is suspiciously close to one year, indicating that it might be an artefact of the data reduction. We therefore discuss the results obtained from the 3-planet model in the rest of this section.

Adopting the 3-planet model, the estimated parameter values are listed in Table 10 while the 1-D marginalised posterior probability distributions are shown in Fig. 4. The mean RV curve for the 4-planet model is overlaid on the RV measurements in Fig. 3.

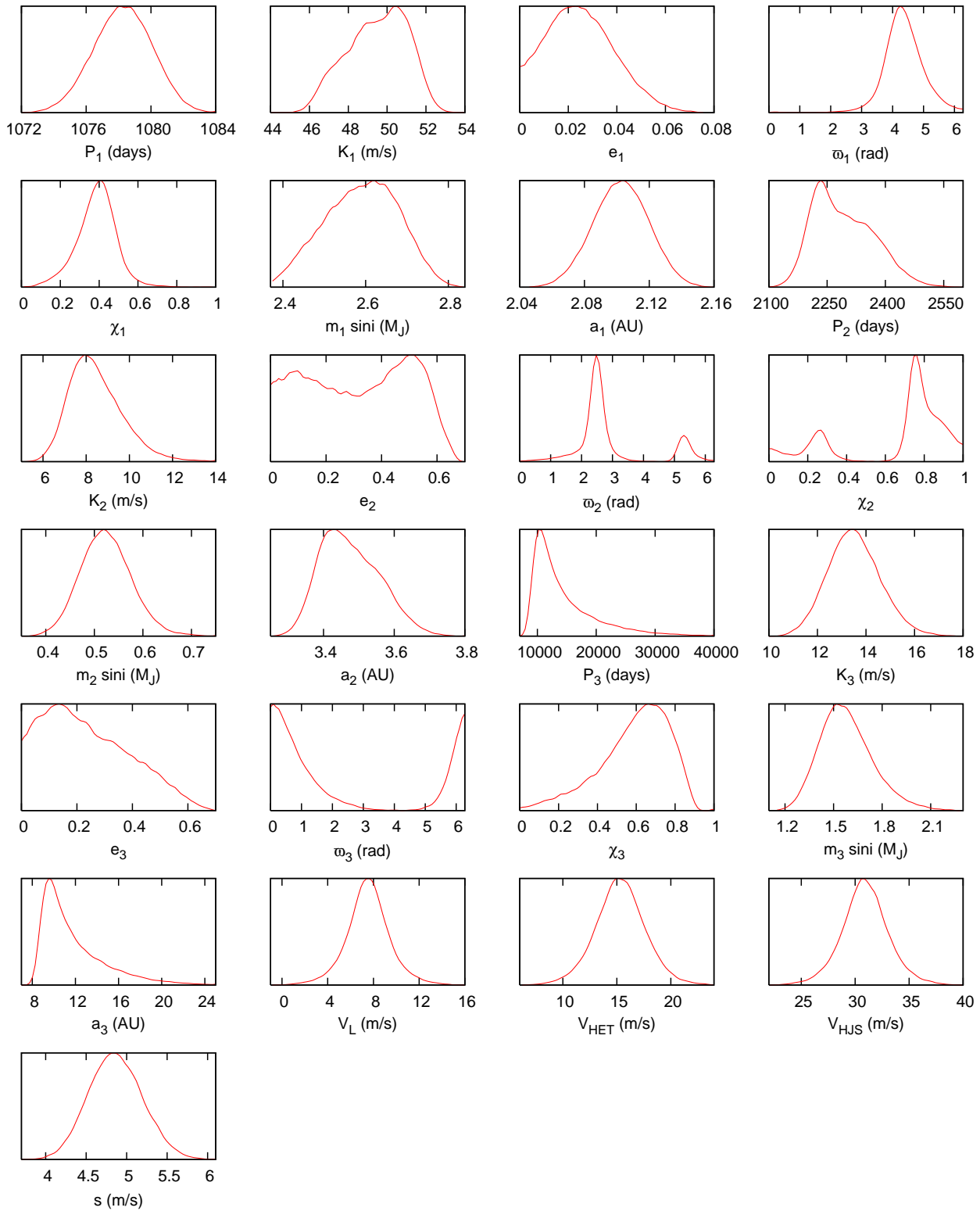


Figure 4. 1-D marginalised posterior probability distributions for the parameters of the three planets found orbiting 47 Ursae Majoris.

Parameter	47 UMa b	47 UMa c	47 UMa d
P (days)	1078.26 ± 1.83 (1078.69)	2293.17 ± 79.39 (2228.61)	14674.55 ± 5925.37 (17217.04)
K (m/s)	49.49 ± 1.53 (51.22)	8.49 ± 1.30 (10.18)	13.52 ± 1.09 (13.42)
e	0.03 ± 0.01 (0.04)	0.32 ± 0.18 (0.55)	0.24 ± 0.16 (0.36)
ϖ (rad)	4.32 ± 0.74 (4.29)	2.95 ± 1.32 (2.42)	2.37 ± 2.37 (0.32)
χ	0.39 ± 0.11 (0.41)	0.64 ± 0.28 (0.75)	0.58 ± 0.19 (0.69)
$m \sin i$ (M_J)	2.59 ± 0.09 (2.71)	0.53 ± 0.05 (0.57)	1.58 ± 0.17 (1.66)
a (AU)	2.10 ± 0.02 (2.11)	3.48 ± 0.08 (3.43)	11.81 ± 2.99 (13.40)

Table 10. Estimated parameter values for the three planets found orbiting 47 Ursae Majoris. The estimated values are quoted as $\mu \pm \sigma$ where μ and σ are the posterior mean and standard deviation respectively. The numbers in parentheses are the maximum-likelihood parameter values.

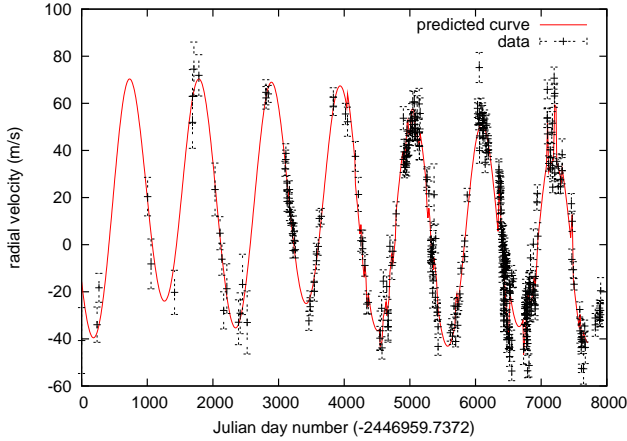


Figure 3. Radial velocity measurements, with 1σ errorbars, and the mean fitted radial velocity curve with three planets for 47 Ursae Majoris.

There is fairly good agreement between our parameter constraints and those presented by Gregory & Fischer (2010).

7.3 HD 10180

HD 10180 is a G1 V type star at a distance of 39 pc with mass $1.06 \pm 0.05 M_{\odot}$ (Lovis et al. 2010). Using the RV data from HARPS instrument (Mayor 2003), Lovis et al. (2010) recently reported at least five and as many as seven planets orbiting this star. There has been much interest in the possible seventh planet as its minimum mass as reported by Lovis et al. (2010) is $1.4 M_{\oplus}$. We analyse the same HARPS data-set after subtracting a mean radial velocity of 3.55302 km/s from it. The resultant RV data is plotted in Fig. 6.

The evidence and jitter values are presented in Table 11. We can clearly see $N_p = 6$ is the favoured model, with the residual evidence ratio strongly implying that the residual data consists of noise only. Adopting the 6-planet model, the estimated parameter values are listed in Table 12 while the 1-D marginalised posterior probability distributions are shown in Fig. 5. The mean RV curve for the 6-planet model is overlaid on the RV measurements in Fig. 6. It can

N_p	$\Delta \ln \mathcal{Z}_r$	s (m/s)
1	24.84 ± 0.17	5.64 ± 0.29
2	9.46 ± 0.18	4.55 ± 0.23
3	63.47 ± 0.17	3.96 ± 0.20
4	45.47 ± 0.17	2.45 ± 0.13
5	4.49 ± 0.17	1.58 ± 0.09
6	-0.73 ± 0.17	1.36 ± 0.07

Table 11. The evidence and jitter values for the system HD 10180.

be seen that our orbital parameters are in general reasonably good agreement with the ones presented in Lovis et al. (2010).

Lovis et al. (2010) found fairly strong peaks with periods 1.178 and 6.51 days in the periodogram of the residuals of the 6-planet Keplerian model. They noted that these two peaks are aliases of each other with 1 sidereal day period ($|1/6.51 - 1.0027| \approx 1/1.178$). Arguing that it is unlikely for the system to be dynamically stable with two planets having $P = 5.76$ days and $P = 6.51$ days, they concluded that if the 7th signal is caused by a planet, it is likely to have $P = 1.178$ days. Meanwhile, they were not able to rule out conclusively or confirm the presence of the 7th planet. Our analysis of the residual data of the 6-planet model did reveal several peaks in the posterior distribution with periods around 6.51 and 1 days, but as can be seen from the value of residual evidence in Tab. 11, they were not found to be sufficiently significant. We therefore rule out the presence of any additional planets contributing to the RV data.

8 CONCLUSIONS

We have presented a new and efficient method to detect extrasolar planets from RV measurements. Our method is not only able to fit for a specific number of planets, but can also infer the number of planets from the data using Bayesian model selection. We have successfully applied our method to simulated data-sets, as well as to the real systems HD 37124, 47 Ursae Majoris and HD 10180. Our method can potentially identify many undiscovered extrasolar planets in existing RV data-sets. One drawback of our method is that it ignores the planet-planet interactions, but these interactions

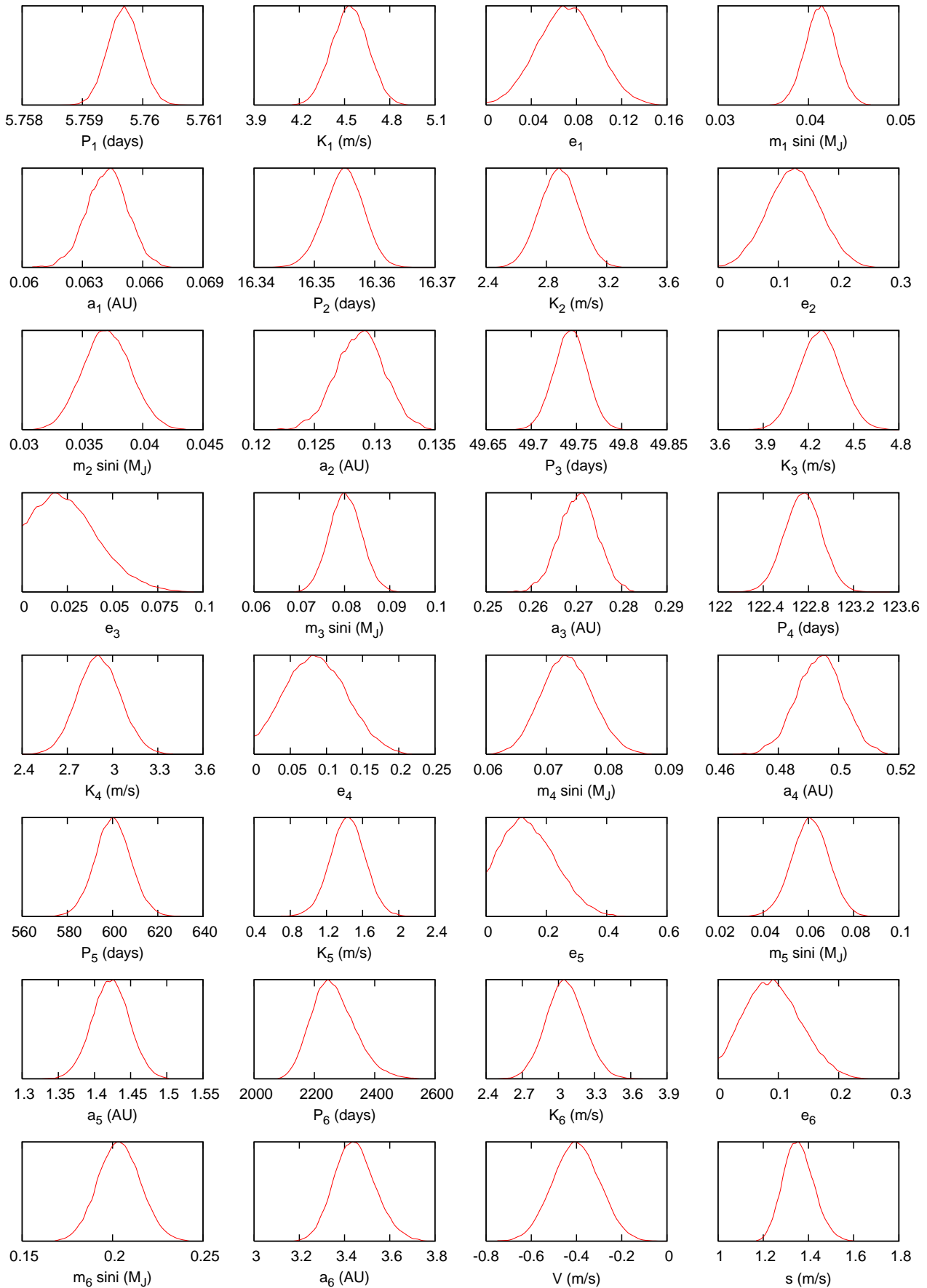


Figure 5. 1-D marginalised posterior probability distributions for the parameters of the six planets found orbiting HD 10180.

Parameter	HD 10180 b	HD 10180 c	HD 10180 d	HD 10180 e	HD 10180 f	HD 10180 g
P (days)	5.76 ± 0.02 (5.76)	16.35 ± 0.05 (16.36)	49.74 ± 0.20 (49.74)	122.75 ± 0.54 (122.69)	600.17 ± 13.75 (601.88)	2266.22 ± 412.42 (2231.44)
K (m/s)	4.54 ± 0.12 (4.63)	2.89 ± 0.13 (2.94)	4.28 ± 0.14 (4.25)	2.91 ± 0.14 (2.70)	1.43 ± 0.20 (1.79)	3.06 ± 0.16 (2.98)
e	0.07 ± 0.03 (0.08)	0.13 ± 0.04 (0.12)	0.03 ± 0.02 (0.03)	0.09 ± 0.04 (0.08)	0.15 ± 0.09 (0.25)	0.09 ± 0.05 (0.05)
ϖ (rad)	2.60 ± 0.38 (2.51)	2.62 ± 0.35 (2.49)	2.56 ± 0.16 (5.12)	2.65 ± 0.53 (2.95)	3.08 ± 0.97 (2.43)	2.89 ± 2.60 (5.98)
χ	0.22 ± 0.06 (0.24)	0.35 ± 0.06 (0.37)	0.43 ± 0.27 (0.83)	0.23 ± 0.11 (0.16)	0.31 ± 0.28 (0.27)	0.67 ± 0.10 (0.73)
$m \sin i$ (M_J)	0.04 ± 0.00 (0.04)	0.04 ± 0.00 (0.04)	0.08 ± 0.00 (0.08)	0.07 ± 0.00 (0.07)	0.06 ± 0.00 (0.07)	0.20 ± 0.01 (0.20)
a (AU)	0.06 ± 0.00 (0.06)	0.13 ± 0.00 (0.13)	0.27 ± 0.00 (0.27)	0.49 ± 0.00 (0.49)	1.42 ± 0.03 (1.42)	3.45 ± 0.16 (3.40)

Table 12. Estimated parameter values for the six planets found orbiting HD 10180. The estimated values are quoted as $\mu \pm \sigma$ where μ and σ are the posterior mean and standard deviation respectively. The numbers in parenthesis are the maximum-likelihood parameter values.

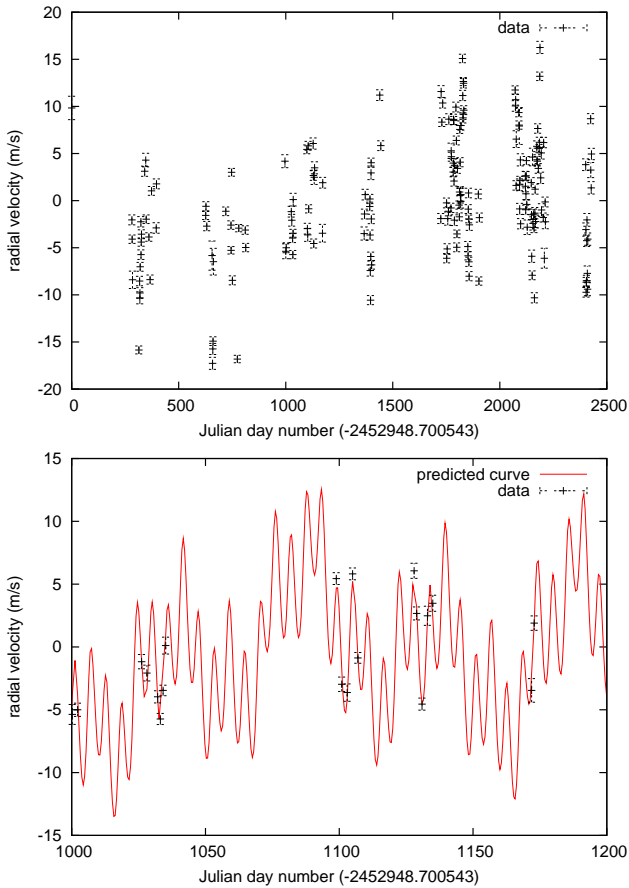


Figure 6. Top panel shows the radial velocity measurements (after subtracting mean RV of 3.55302 km/s), with 1σ errorbars. Bottom panel shows a blow-up of the mean fitted radial velocity curve with six planets for HD 10180.

are important only for a very small fraction of planetary systems. Moreover, our basic methodology can be extended to include such interactions. This will be undertaken in further work.

Another important avenue of research in extrasolar planet searches is to perform a coherent analysis using different data-sets,

e.g. by jointly analysing the RV data and light curves for the same system. This would enable us to place better constraints on the planetary parameters and also to learn about the physical structure of the planets. Once again our basic analysis technique can be easily extended to perform a joint analysis of data sets of different types. We plan to extend our approach by incorporating light curve data in a forthcoming paper.

ACKNOWLEDGEMENTS

We would like to thank the referee, Phil Gregory, for useful comments on the paper and Pedro Carvalho for useful discussions regarding multiple object detection. This work was carried out largely on the COSMOS UK National Cosmology Supercomputer at DAMTP, Cambridge and the Darwin Supercomputer of the University of Cambridge High Performance Computing Service (<http://www.hpc.cam.ac.uk/>), provided by Dell Inc. using Strategic Research Infrastructure Funding from the Higher Education Funding Council for England. FF is supported by a Research Fellowship from Trinity Hall, Cambridge. STB acknowledges support from the Isaac Newton Studentship.

REFERENCES

- Balan S. T., Lahav O., 2009, MNRAS, 394, 1936
 Butler R. P., Marcy G. W., 1996, ApJ, 464, L153+
 Butler R. P., Marcy G. W., Vogt S. S., Fischer D. A., Henry G. W., Laughlin G., Wright J. T., 2003, ApJ, 582, 455
 Butler R. P., Wright J. T., Marcy G. W., Fischer D. A., Vogt S. S., Tinney C. G., Jones H. R. A., Carter B. D., Johnson J. A., McCarthy C., Penny A. J., 2006, ApJ, 646, 505
 Clyde M. A., Berger J. O., Bullard F., Ford E. B., Jefferys W. H., Luo R., Paulo R., Loredo T., 2007, in G. J. Babu & E. D. Feigelson ed., Statistical Challenges in Modern Astronomy IV Vol. 371 of Astronomical Society of the Pacific Conference Series, Current Challenges in Bayesian Model Choice. pp 224+
 Feroz F., Gair J. R., Hobson M. P., Porter E. K., 2009a, Classical and Quantum Gravity, 26, 215003
 Feroz F., Hobson M. P., 2008, MNRAS, 384, 449
 Feroz F., Hobson M. P., Bridges M., 2009b, MNRAS, 398, 1601

- Feroz F., Hobson M. P., Zwart J. T. L., Saunders R. D. E., Grainge K. J. B., 2009c, MNRAS, 398, 2049
- Feroz F., Marshall P. J., Hobson M. P., 2008, ArXiv e-prints [arXiv:0810.0781]
- Fischer D. A., Marcy G. W., Butler R. P., Laughlin G., Vogt S. S., 2002, ApJ, 564, 1028
- Ford E. B., 2005, AJ, 129, 1706
- Ford E. B., Gregory P. C., 2007, in G. J. Babu & E. D. Feigelson ed., Statistical Challenges in Modern Astronomy IV Vol. 371 of Astronomical Society of the Pacific Conference Series, Bayesian Model Selection and Extrasolar Planet Detection. pp 189–+
- Goździewski K., Konacki M., Maciejewski A. J., 2006, ApJ, 645, 688
- Gregory P. C., 2005, ApJ, 631, 1198
- Gregory P. C., 2007a, MNRAS, 374, 1321
- Gregory P. C., 2007b, MNRAS, 381, 1607
- Gregory P. C., Fischer D. A., 2010, MNRAS, 403, 731
- Hobson M. P., McLachlan C., 2003, MNRAS, 338, 765
- Liddle A. R., 2007, MNRAS, 377, L74
- Lomb N. R., 1976, Ap&SS, 39, 447
- Lovis C., Ségransan D., Mayor M., Udry S., Benz W., Bertaux J., Bouchy F., Correia A. C. M., Laskar J., Lo Curto G., Morasini C., Pepe F., Queloz D., Santos N. C., 2010, ArXiv e-prints [arXiv:1011.4994]
- Mackay D. J. C., 2003, Information Theory, Inference and Learning Algorithms. Cambridge University Press, Cambridge, UK
- Mayor M. e. a., 2003, The Messenger, 114, 20
- Scargle J. D., 1982, ApJ, 263, 835
- Skilling J., 2004, in Fischer R., Preuss R., Toussaint U. V., eds, American Institute of Physics Conference Series Nested Sampling. pp 395–405
- Takeda G., Ford E. B., Sills A., Rasio F. A., Fischer D. A., Valenti J. A., 2007, ApJS, 168, 297
- Trotta R., 2007, MNRAS, 378, 72
- Tuomi M., Kotiranta S., 2009, A&A, 496, L13
- Valenti J. A., Fischer D. A., 2005, ApJS, 159, 141
- Vogt S. S., Butler R. P., Marcy G. W., Fischer D. A., Henry G. W., Laughlin G., Wright J. T., Johnson J. A., 2005, ApJ, 632, 638
- Vogt S. S., Marcy G. W., Butler R. P., Apps K., 2000, ApJ, 536, 902
- Wittenmyer R. A., Endl M., Cochran W. D., Levison H. F., Henry G. W., 2009, ApJS, 182, 97